

# A Comparison on Efficiency of Triangular and Orthogonal Arrays in Determination of Shear Wave Velocity Profile of the Layers Close to the Earth Surface using F-K Method

Mohammad Davoodi\*, Ebrahim Haghshenas, Mohammad Kazem Jafari  
and Mehran Esfahanizadeh

Department of Geotechnical Engineering, International Institute of Earthquake Engineering and Seismology (IIEES),  
Tehran, Iran; m-davood@iiees.ac.ir, haghshen@iiees.ac.ir, jafari@iiees.ac.ir, mehesf@yahoo.com

## Abstract

In order to assess and compare efficiency of triangular and orthogonal arrays in identification of subsurface structure specifications up to a depth of 50 meters using microtremor waves by F-K method, two triangular and orthogonal arrays with 13 and 12 stations (which included some sub-arrays), respectively, were studied in a site located in north of Iran and besides the Caspian Sea called Kalarabad. Data acquisition in these arrays was carried out using three-component seismographs with minimum and maximum distance of 5 meters and 70 meters, respectively, for at least 18 continuous hours. In the mentioned site, dominant layering was saturated and poorly graded sandstone and shear wave velocity profile was formerly determined for a depth up to 50 meters by Down Hole method. Natural and dominant frequency of the site was obtained as much as 0.33 by H/V analyses. The dispersion curves obtained through processing each of sub-arrays were extracted and then compared with the dispersion curve obtained through shear wave velocity profile of Down Hole. This comparison indicated better efficiency of orthogonal arrays in the mentioned site. Also, azimuth direction of wave propagation was assessed in this site and the corresponding effects on subsurface structure identifiable ranges were studied in triangular and orthogonal arrays along with theoretical response for each form.

**Keywords:** Arrays, Dispersion Curve, F-K Method, Microtremor, Shear Wave Velocity Profile

## 1. Introduction

Nowadays, use of microtremor wave's array method has been widely expanded in determination of shear wave velocity profile of subsurface layers. Dimensions and distances of arrays are effective on determination of the depth to be identified and the arrays with small dimensions are typically used to identify the layers near the earth surface<sup>1</sup>.

The shape of used arrays are also so variant and triangular, circular, semi-circular, orthogonal, spiral forms can

be taken into account as the most conventional ones for array arrangement. At the field operations in particular urban areas, use of each form depends on spatial restrictions on establishment of array stations and despite of attractions for using circular and semi-circular arrays, triangular or orthogonal arrays are occasionally enforced to be used<sup>2</sup>. So far, several processing approaches have been presented including F-K, SPAC, ESPAC, MSPAC, etc.<sup>3</sup> each of which can estimate the site-specifications such as dispersion curve and/or spatial autocorrelation curve based on specific assumptions and the regarding

\*Author for correspondence

mathematical relations which are associated with vertical component records of microtremor waves (obtained from the seismographs employed in the array) and the array geometry<sup>4</sup>.

The present study tried to investigate efficiency of triangular and orthogonal arrays using F-K processing method in determination of shear wave velocity of the site besides the earth surface (up to a depth of 50 meters).

### 1.1 The Site-Specifications

The studied site is located in north of Iran and south of Caspian Sea with latitude of 36 41 57 degrees and longitude of 51 15 47 degrees as well as an approximate distance of 200 meters from beach in south side of the main road in Mazandaran province. Satellite map of the site area is shown in Figure 1 along with the soil layering profile and mean numbers curve of NSPT. In this site, totally 6 test holes with different depths- with a maximum digging depth of 70 meters- and 3 down hole tests were carried out at the preliminary and complementary geotechnical identification phase. According to these studies, the desired land is composed of 4 single layers up to the depth of 70 meters in so far as the first layer is mostly formed loose poorly graded Sandstone (SP) with a thickness of 8 meters, the second layer owns low-plasticity clay with silt (CL) with a thickness of 6 meters, the third layer contains moderately dense Clayey Sandstone (SC) with a thickness of 6 meters and the fourth layer consists of dense poorly graded sandstone with CL interbedded (SP)

and thickness of above 50 meters. Groundwater level was also observed at the depth of 6 meters. Shear wave velocity profile obtained from Down Hole Test and the corresponding dispersion curves are depicted in Figure 2.

### 1.2 The Arrays Properties

At the desired site, two triangular and orthogonal arrays with 13 and 12 stations, respectively, were located using 3-component seismograph CMG-6TD-GURALP for at least 18 continuous hours within 2 days with similar climate and traffic conditions. Sampling frequency was 100 sps at all measurements and in order to allow measurements overlapping with the least possible error, each receiver was connected to a GPS. In triangular array, the closest and furthest distance between stations were  $D_{min} = 5.m$  and  $D_{max} = 69.3m$ , respectively while they were  $D_{min} = 10.m$  and  $D_{max} = 60.m$  in orthogonal array. Figure 3 shows the arrangement style per array. The mentioned triangular array can be considered with 13 sub-arrays as well as at least 4 stations and at most 13 stations. Besides, orthogonal array can be taken into consideration with 15 sub-arrays as well as at least 3 stations and at most 12 stations.

## 2. Data Processing

Since the records were logged continuously for more than 18 hours, these records were initially separated as one-hour timescales and the obtained mappings were

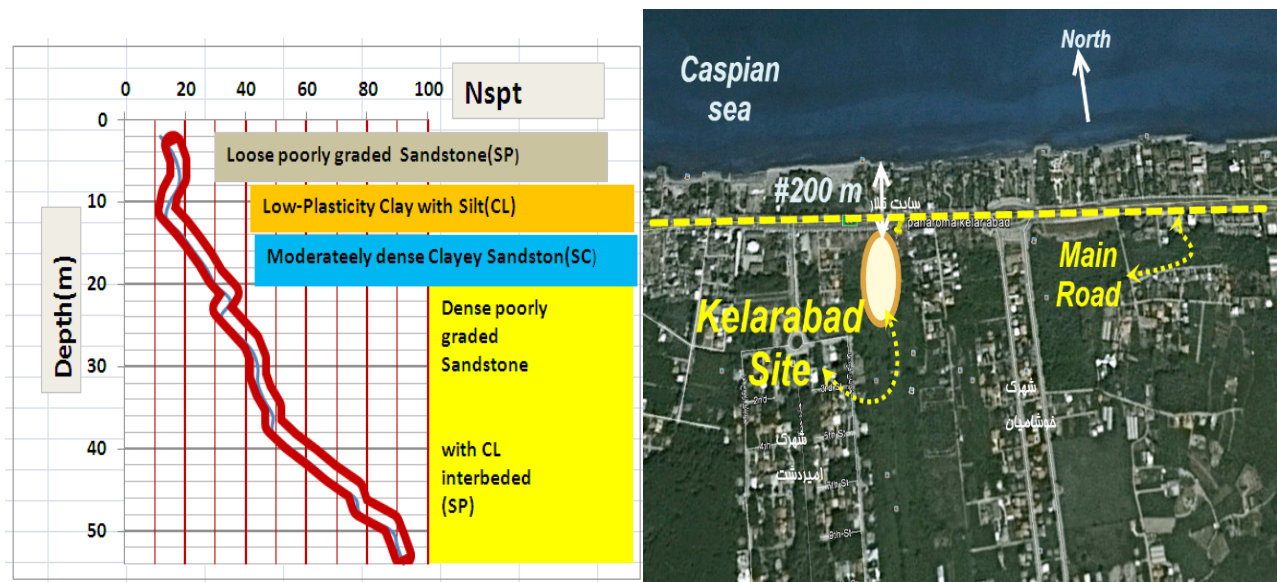


Figure 1. Satellite map of Kelarabad Site, the soil layering profile and NSPT number range at depth.

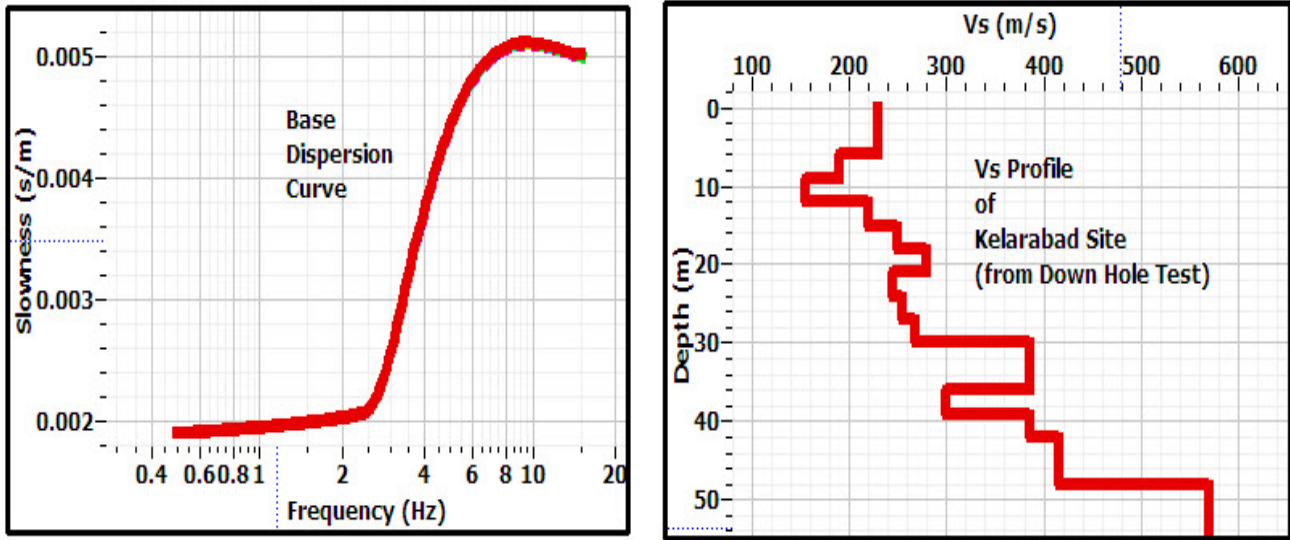


Figure 2. Shear wave velocity profile at the depth along with the corresponding dispersion curve.

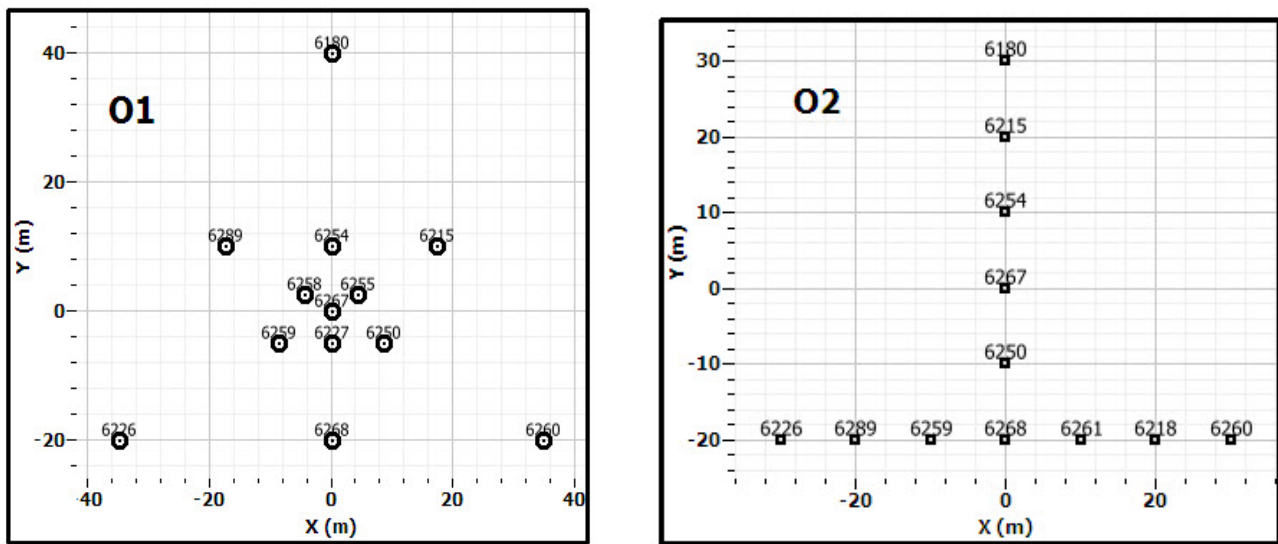


Figure 3. Triangular and orthogonal arrays arrangement plan in Kelarabad site.

compared to ensure devices performance which indicated stationary mappings. In doing so, single-station analysis was carried out using Nakamura method<sup>5</sup>. Figure 4 shows H/V analysis results related to 13 triangular array stations. Given the conducted analyses at all stations located in Kelarabad site, the dominant frequency in 13 stations were estimated about 0.33 Hz which can be evaluated as the site dominant frequency. In this frequency, the magnification greater than 4 and small standard deviations were acceptable. According to these results, Kelarabad site is argued to be placed in category of low natural

frequency sites thereby these processes reveal the devices performance conformity as well as parallel and almost homogenous layers assumptions achievement in the site. As mentioned earlier, data processing and dispersion curve extraction by F-K method was considered in present paper. This method has been widely used by various researchers, such as<sup>3,6-33</sup>.

In conventional F-K method, a high quality dispersion curve can be obtained by adjustment of opening and distance between the stations with desired wavelength range (from shorty to long wavelength)<sup>34</sup>. In this method,

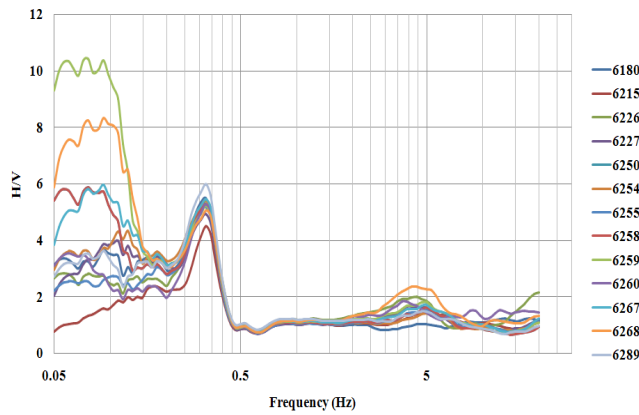


Figure 4. Single-station analysis results by Nakamura method for 13 stations located in Kelarabad site.

restricted array opening can decrease separation ability in low frequencies. For instance, lack of proper separation ability can cause some problems to gain wave number from F-K range in low frequencies particularly in case of multiple wave sources which get the station from different directions (Wood and Lintz, 1973). The separation limits of an array are controlled by the minimum wave number ( $K_{min}$ ) which itself depends upon the geometry and the maximum opening of array.

In present study, the records processing was carried out using the software Sesarray in order to reach dispersion curve and shear wave velocity profile by F-K method<sup>32</sup>. At Build-Array section of mentioned software, theoretical response of each triangular and orthogonal sub-array was extracted and based on which maximum and minimum wavenumbers ( $K_{max}$ ,  $K_{min}$ ) and wavelengths ( $\lambda_{max}$ ,  $\lambda_{min}$ ) were determined which could be identified according to geometrical properties of sub-arrays. Tables 1 and 2 present a summary of these results along with geometrical properties of each sub-array for triangular and orthogonal forms, respectively.

$K_{Min}/2$  and  $K_{Max}$  values in above Tables are controller values per different azimuth directions. In other words,  $K_{Min}/2$  is the greatest  $K_{Min}/2$  among different directions in the table and  $K_{Max}$  is the lowest  $K_{Max}$  in the table associated with different directions of wave propagation. These values were also extracted per different directions and as addressed by other researchers as well,  $K_{Min}/2$  values are wave propagation-independent triangular arrays therefore in orthogonal arrays; this value is sensitive to the propagation angle. According to this issue, single-station analysis was carried out by H/V Rotate method using three-component mappings from the site<sup>33</sup>. The final

Table 1. Triangular arrays properties and maximum and minimum values for wave number and wavelength as the theoretical response of array

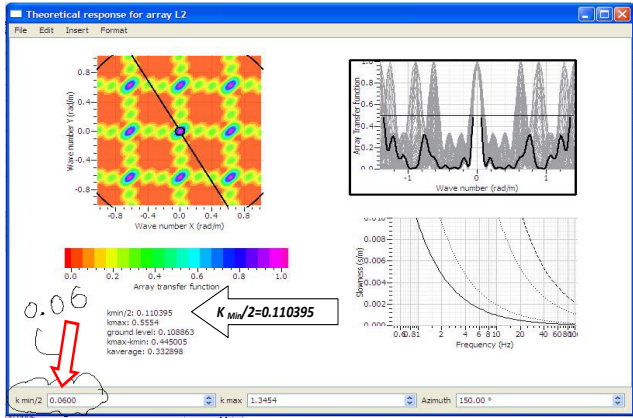
Array Name	NO Sensor	D Min	D Max	DMax /DMin	K Min/2	K Max	$\lambda$ Max	$\lambda$ Min	$\Delta\lambda$
A1	4	5	8.6	1.72	0.265	1.19	23.66	5.29	18.37
B1	4	10	17.3	1.73	0.133	0.59	47.33	10.59	36.74
C1	4	20	34.6	1.73	0.066	0.3	94.66	21.17	73.49
D1	4	40	69.3	1.73	0.033	0.15	189.32	42.35	147
E1	7	5	17.3	3.46	0.159	0.76	39.63	8.32	31.31
F1	7	10	34.6	3.46	0.079	0.38	79.26	16.64	62.62
G1	7	20	69.3	3.46	0.04	0.19	158.53	33.28	125.2
H1	7	5	34.6	6.92	0.089	1.08	70.82	5.8	65.02
I1	7	5	69.3	13.86	0.046	0.14	136.76	44.72	92.04
K1	7	10	69.3	6.93	0.044	0.54	141.65	11.6	130
M1	10	10	69.3	6.93	0.047	0.39	132.63	16.25	116.4
N1	10	5	34.6	6.92	0.095	0.77	66.31	8.13	58.19
O1	13	5	69.3	13.86	0.055	0.8	113.35	7.88	105.5

Table 2. Orthogonal arrays properties and maximum and minimum values for wave number and wavelength as the theoretical response of array

Name	N	Dmin	Dmax	Dmax/Dmin	Kmin/2	Kmax	$\lambda_{max}$	$\lambda_{min}$	$\Delta\lambda$
A2	4	10	20	2	0.191	0.44	32.88	14.37	18.52
B2	7	10	40	4	0.143	0.36	43.96	17.27	26.69
C2	10	10	40	4	0.085	0.54	73.67	11.57	62.1
D2	3	10	14.2	1.42	0.24	0.46	26.22	13.70	12.52
E2	3	20	28.5	1.42	0.12	0.23	52.44	27.40	25.04
F2	3	30	42.4	1.42	0.08	0.15	78.66	41.11	37.55
G2	3	30	50	1.67	0.072	0.11	87.49	54.78	32.7
H2	3	30	58.3	1.94	0.069	0.09	91.24	68.49	22.76
I2	5	10	28.5	2.85	0.152	0.53	41.32	11.94	29.38
J2	5	10	42.4	4.24	0.094	0.39	67.15	15.99	51.16
K2	5	10	42.4	4.24	0.107	0.2	58.92	31.91	27.02
L2	7	10	42.4	4.24	0.11	0.56	56.91	11.31	45.6
M2	8	10	50	5	0.102	0.55	61.37	11.39	49.98
N2	9	10	58.3	5.83	0.101	0.55	61.94	11.47	50.47
O2	12	10	60	6	0.055	0.57	114.85	10.95	103.9

result of mentioned processing indicates predominant direction of about 150 degrees for microtremor wave's propagation. Therefore, theoretical response of orthogonal arrays was extracted for above azimuth which is shown in Figure 5 as the sample for array L2. As it can be seen,  $K_{Min}/2$  value was decreased from 0.11 to 0.06 which means increased  $\lambda_{max}$  from 114 meters to 210 meters and as it will be discussed in the next section, it is in line with the corresponding value obtained from array processing.

Since array method is based on mapping the vertical component of Rayleigh waves and its field operations



**Figure 5.** Theoretical response of L2 orthogonal array in azimuth direction of 150 degrees, microtremor waves propagation.

are possible by employment of single-component equipment<sup>4</sup>, it is noteworthy to recommend that in case of sensitive array arrangement to azimuth direction, at least one 3-component device is necessary to be used in order to determine dominant direction of microtremor waves propagation and extract the resulted valued from theoretical response for mentioned azimuth and thereafter to use and compare them. In this regard, greater depth ranges can be identified compared to subsurface structure.

Figure 6 shows the obtained dispersion curve for the sub-array E1 in four selected hours 03:00, 09:00, 15:00 and

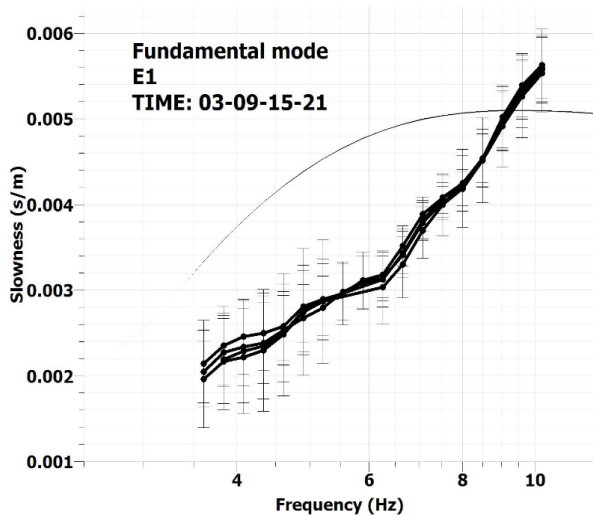


**Figure 6.** Dispersion curve of triangular array for 7 stations in four selected hours 03:00, 09:00, 15:00 and 21:00 in local time.

21:00. According to proper fitness of dispersion curves in different hours and lower noise at 03:00 a.m. local time, the processes associated with the hour 03:00 a.m. were considered as the selected time in results comparison.

Figure 7 depicts dispersion curve of two triangular (O1) and orthogonal (O2) arrays relative to dispersion curve spectrum of an appropriate parametric model of layering and layers shear wave velocity. Misfit value which was calculated from Equation 1 (based on Figure 8<sup>28</sup>) by the software was shown as about 0.07 for both arrays which indicates appropriateness of the selected parametric model. Nevertheless, this does not mean fitness of shear wave velocity profile obtained from regression analysis with base profile of the site. Since regression analysis may cause some errors or uncertainties in estimation of shear wave velocity profile, comparison can be referred to the prior stage of regression analysis and thereby compare fitness of dispersion curve obtained from processes with the corresponding dispersion curve of the base profile (obtained from Down-Hole Test).

Therefore, the next figures show dispersion curve related to the sub-arrays along with the corresponding dispersion curve with the base dispersion curve. Figures 9 and 10 depict dispersion curve of 7-station triangular sub-arrays and dispersion curve of 10-station triangular sub-arrays, respectively.

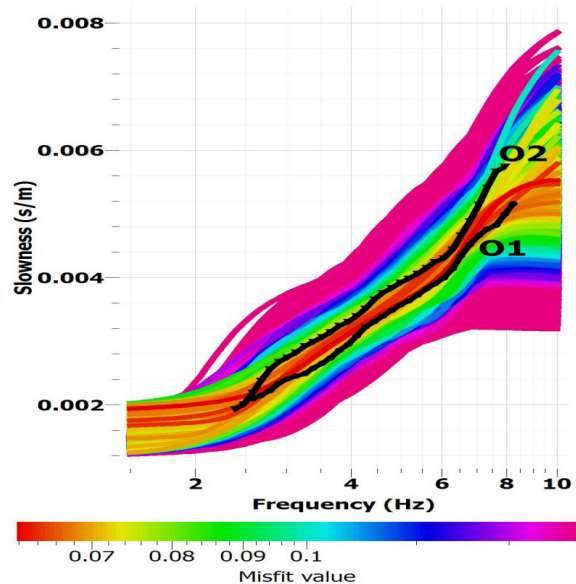


**Figure 7.** The comparison on dispersion curve of triangular (O1) and orthogonal (O2) arrays with dispersion curve spectrum of the appropriate parametric model.

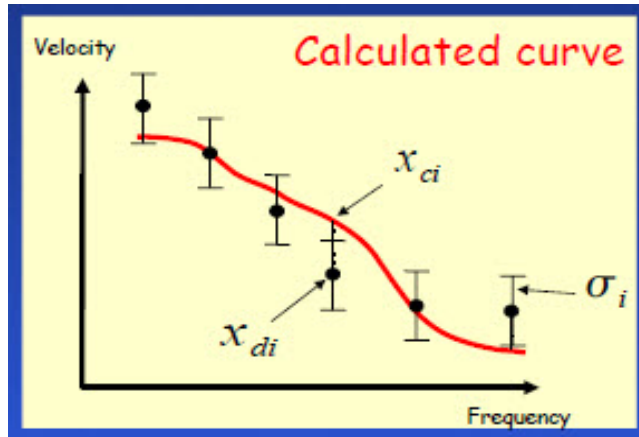


Figure 8.

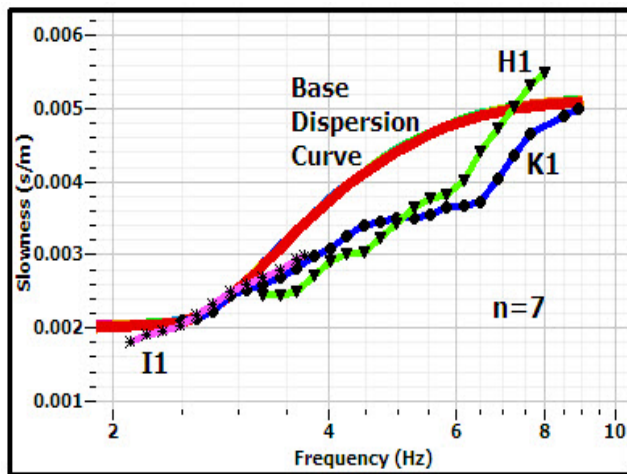


Figure 9. Dispersion curve of 7-station triangular sub-arrays compared to the base profile.

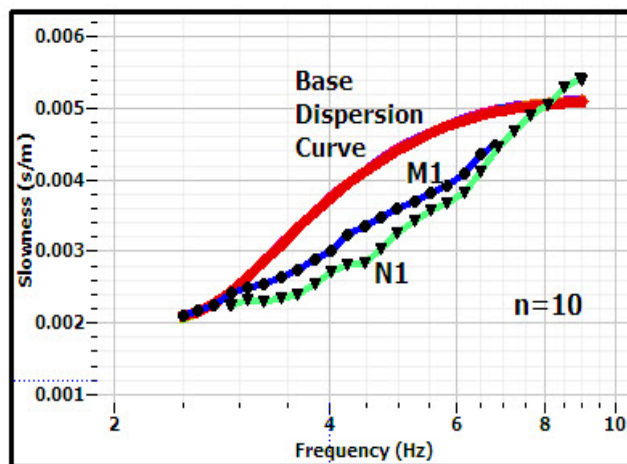


Figure 10. Dispersion curve of 10-station triangular sub-arrays compared to the base profile.

The dispersion curve obtained from 5-station orthogonal sub-arrays is shown in Figure 11 and that of 8-9-10- and 12-station orthogonal sub-arrays is depicted in Figure 12. Furthermore, dispersion curves of 4-station triangular arrays and 3- and 4-station orthogonal arrays had no appropriate fitness with the base profile.

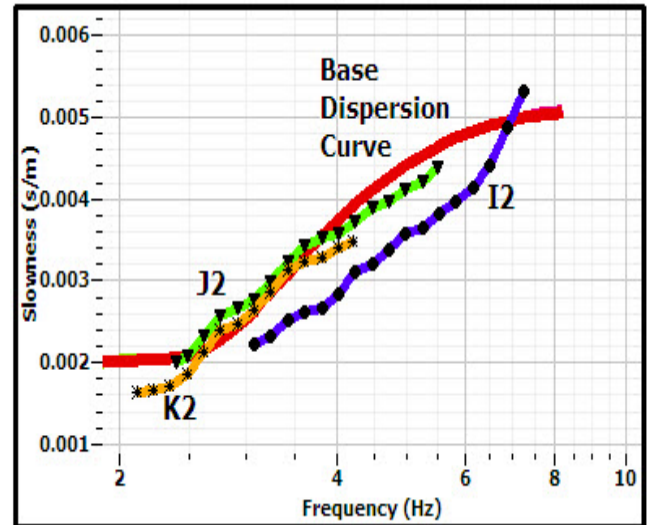


Figure 11. Dispersion curve of 5-station orthogonal sub-arrays compared to the base profile.

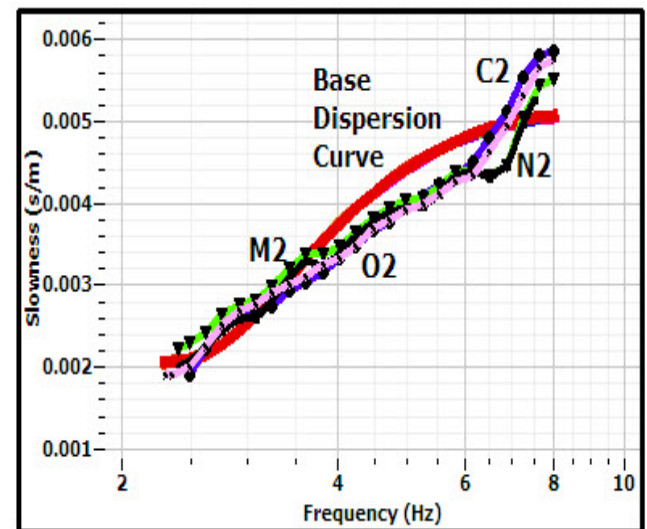
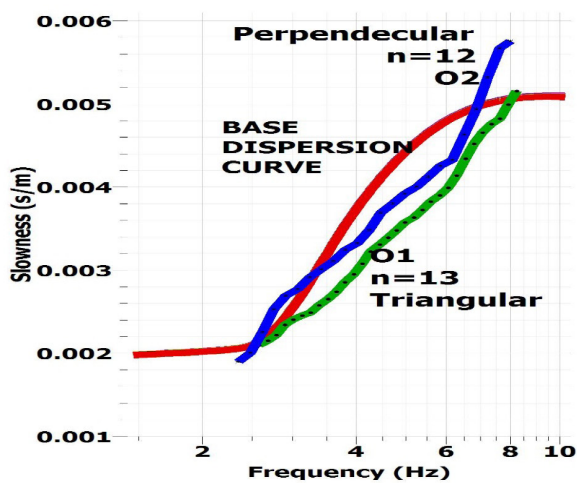


Figure 12. Dispersion curve of 8-, 9-, 10- and 12-station orthogonal sub-arrays compared to the base profile.

### 3. Discussion

As it can be seen from Tables 1 and 2, minimum and maximum values for the wavelength related to each array

was calculated according to wave number resulted from the theoretical response. Also, according to uncertainty in extraction of precise shear wave velocity profile, achievement of what a wavelength range identified by measurements done at each stage is of high importance. Definitely, the lower identified minimum wavelength and the greater identified maximum wavelength, the higher potential for array in the soil profile determination. The corresponding identification depth of received information from each wavelength for low depths is conventionally considered as much as one third of the wavelength (Sebastiano Foti, 2000). Therefore, the velocity profiles resulted from inversion process will not be validated within the range lower than the corresponding depth of minimum wavelength ( $\lambda_{\min}$ ) and greater than the corresponding depth of maximum wavelength ( $\lambda_{\max}$ ). These values can be readily calculated for any arrays and any processing practice by reading frequency and slowness at the beginning and end of extracted dispersion curve. Consequently, another important note here is the fitness of obtained curve with the specific-site curve where calculated misfit values per process relative to the specific-site curve can quantitatively indicate the mentioned fitness. Dispersion curve of two arrays including O1 (triangular with 13 stations) and O2 (orthogonal with 12 stations) in comparison to dispersion spectrum of the parametric model was presented formerly in Figure 7 and Figure 13 depicts the comparison of these two curves compared to the base dispersion curve.



**Figure 13.** Comparison between dispersion curve of two arrays including O1 (triangular) and O2 (orthogonal) and the base dispersion curve.

These two arrays own an approximately similar frequency range of 2-8 Hz so that according to equal slowness in frequency of 2 Hz and a relative equivalence in the frequency of 8 Hz, both arrays offer maximum and minimum wavelength as 200 meters and 23.5 meters, respectively, which may be useful for identification of the depth of 7 to 70 meters. Therefore, as it can be seen in terms of fitness with the base profile, the array O2 has better conditions and misfit values for two arrays O1 and O2 relative to the base profile are 1.26 and 0.85, respectively, which quantitatively address better fitness of the array O2 in F-K method. As it was seen from Figure 7, these two arrays were applied in a parametric model where misfit value was obtained lower than 0.07 which indicates inappropriateness of parametric model to compare fitness and efficiency of two arrays. Minimum and maximum distance of the array O1 were 5 meters and 69.3 meters, respectively, while they were 10 meters and 60 meters, respectively, in the array O2. However, although O2 orthogonal array has more limited dimensions compared to O1 triangular array, it shows a better efficiency and fitness which addresses excellence of orthogonal arrangement in comparison with triangular one in F-K method. As another instance in Figure 14, F1 triangular array and L2 orthogonal array (each with 7 stations and maximum distances of 34.6 meters and 42.4 meters, respectively) were compared. This comparison also indicated better efficiency of orthogonal array in this method. Misfit values of F1 triangular array and L2 orthogonal array relative to the base dispersion curve were obtained 1.62 and 1.06, respectively.

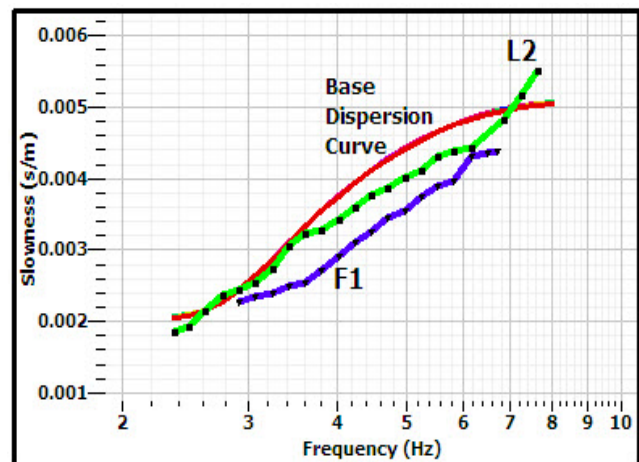


**Figure 14.** The comparison between dispersion curve of F1 triangular array and L2 orthogonal array and the base dispersion curve.

Almost at all triangular and orthogonal arrays, the array dispersion curve was placed beneath the base dispersion curve which means estimation of greater velocities in equilibrium depths. This difference is much higher in triangular arrays which offer greater velocities relative to the base shear wave velocity profile (resulted from Down Hole) compared to orthogonal arrays in extracted shear wave velocity profile from regression analysis. The greater shear wave velocity resulted from array method can be due to nonlinear behavior of the soil in different strains. Since the strains made in the soil resulted from microtremors are quite (completely) lower than those in Down Hole Test conditions therefore corresponding velocities in each depth show greater values in array method.

## 4. Conclusion

In Kellarabad site, orthogonal arrays showed a better efficiency compared to triangular ones in the processes conducted by F-K method and even in the arrays with more limited dimensions and lower number of stations, dispersion curve of orthogonal arrays is clearly closer to the base shear wave velocity profile. Also, it can be expected that in the conditions similar with triangular array, orthogonal arrays will show a more appropriate fitness (as much as about 30%) with the site-specific dispersion curve. However, it is noteworthy to consider that triangular arrays have more capabilities to fit with desired geometries of other methods (e.g. SPAC), compared to orthogonal array.

Orthogonal arrays in some of wave propagation direction ranges have such a potential to identify a wider range of subsurface structure depth while triangular arrays are not sensitive to waves propagation azimuth.

In corresponding depths, both triangular and orthogonal forms yield greater shear wave velocity than those obtained from Down Hole Test. However, this difference is higher in triangular arrays and orthogonal arrays estimate more appropriate values.

## 5. Acknowledgements

The authors are grateful to the Geotechnical Department and the Electronic Instrumentation Group of International Institute of Earthquake Engineering and Seismology (IIIES). Arzhan Khak Shomal Co., and Arzhan Arg Co., for geotechnical survey and Down Hole test. Many people greatly contributed to this work. Special mention

goes to Shahm Atashband, HamidReza H. Moghadar, and Hamid Reza Mohammad Yusef for their efforts during the ambient array test.

## 6. References

1. Chouet B, De Luca G, Milana G, Dawson P, Martini M, Scarpa R. Shallow velocity structure of Stromboli Volcano, Italy, derived from small aperture array measurements of Strombolian tremor. *Bull Seism Soc Am.* 1998; 88:653–66.
2. Suetomi I, Nakamura S. Spectral characteristics and nonlinear effects during recent large earthquakes observed at Kushiro City, Japan. *Acapulco, Mexico: 10th World Conference on Earthquake Engineering.* Amsterdam: Elsevier Science, CDROM; 1996.
3. Blind comparisons of shear-wave velocities at closely spaced sites in San Jose, California: U.S. In: Asten MW, Boore editors. *Geological survey open-file report 2005-1169*; 2005. Available from: <http://pubs.usgs.gov/of/2005/1169/>
4. Okada H. *The microseismic survey method: Society of exploration geophysicists of Japan.* Translated by Koya Suto, Geophysical Monograph Series. Tulsa: Society of Exploration Geophysicists; 2003.
5. Haghshenas E, Bard PY, Theodulidis N. Empirical evaluation of microtremor H/V spectral ratio. *SESAME WP04 TEAM. Bull Earthquake Eng.* 2008; 6:75–108.
6. Horike M. Inversion of phase velocity of long-period microtremors to the S-wave-velocity structure down to the basement in urbanized areas. *J Phys Earth.* 1985; 33:59–96.
7. Asten MW, Henstridge JD. Array estimators and the use of microseisms for reconnaissance of sedimentary basins. *Geophysics.* 1984; 49:1828–37.
8. Okada H. A research on long period microtremor array observations and their time and spatial characteristics as probabilistic process, report of a Grant-in-Aid for Co-operative Research. Supported by the Scientific Research Fund in 1985; 1986.
9. Okada H. A research on the practical application of microtremor exploration technique to a wide area survey of a underground structure under 3,000 m in depth, report of a Grant-in-Aid for Co-operative Research. Supported by the Scientific Research Fund in 1993; 1994.
10. Okada H, Matsushima K, Hidaka E. Comparison of spatial autocorrelation method and frequency-wavenumber spectral method of estimating the phase velocity of Rayleigh waves in long-period microtremors. *Geophys Bull Hokkaido Univ.* 1987; 49:53–62.
11. Matsushima T, Okada H. A few remarks on the scheme of observation and analysis in estimating deep geological structures by using long-period microtremors. *Geophys Bull Hokkaido Univ.* 1989; 52:1–10.

12. Sato T, Kawase H, Matsui M, Kataoka S. Array measurement of high frequency microtremors for underground structure estimation. Proc of the 4th International Conference on Seismic Zonation; 1991.
13. Tokimatsu K, Shinzawa K, Kuwayama S, Abe A. Estimation of vs. profiles from Rayleigh wave dispersion data at site affected in the Loma Prieta Earthquake. Stanford, California: Proc of the 4th International Conference on Seismic Zonation. Earthquake Engineering Research Institute. 1991 Aug 25-29; 2:507-14.
14. Tokimatsu K, Miyadera Y, Kuwayama S. Determination of shear wave velocity structures from spectrum analyses of short-period microtremors. Balkema, Rotterdam, Madrid, Spain: Proc 10th World Conference on Earthquake Engineering. 1992 July 19-24; 1:253-8.
15. Tokimatsu K, Shinzawa K, Kuwayama S. Use of short period microtremors for Vs profiling. J Geotech Eng. ASCE. 1992; 118:1544-58.
16. Yamanaka H, Takemura M, Ishida H, Ikeura T, Nozawa T, Sasaki T, Niwa M. Array measurements of long-period microtremors and estimation of S-wave velocity structure in the western part of the Tokyo metropolitan area. J Seism Soc Jpn. 1994; 47:163-72.
17. Miyakoshi K, Okada H. Estimation of the site response in the Kushiro City, Hokkaido, Japan. Using microtremors with seismometer arrays. Acapulco, Mexico: 10th World Conference on Earthquake Engineering. Amsterdam: Elsevier Science, CD-ROM; 1996.
18. Miyakoshi K, Kagawa T, Kinoshita S. Estimation of geological structures under Kobe area using the array recordings of microtremors. In: Irikura K, Kudo K, Okada H, Sasatani T, editors. AA Balkema, Rotterdam: The effects of surface geology on seismic motion; 1998. p. 691-6.
19. Kagawa T, Sawada S, Iwasaki Y, Nanjo A. S-wave velocity structure model of the Osaka sedimentary basin derived from microtremor array observations. Jisin. 1998; 51:31-40.
20. Ishida H, Nozawa T, Niwa M. Estimation of deep surface structure based on phase velocities and spectral ratios of long-period microtremors. The effects of surface geology on seismic motion; 1998.
21. Milana G, Barba S, Del Pezzo E, Zambonelli E. Site response from ambient noise measurements: New perspective from an array study in Central Italy. Bull Seism Soc Am. 1996; 86:320-8.
22. Kataoka S, Kawase H. Estimation of underground structure at Higashinada Ward, Kobe using surface wave of microtremor and explosion record. Jisin. 1998; 51:99-112.
23. Kawase H, Satoh T, Iwata T, Irikura K. SW-wave velocity structure in the San Fernando and Santa Monica areas. The effects of surface geology on seismic motion. In: Irikura K, Kudo K, Okada H, Sasatani T, editors. A. A. Balkema, Rotterdam; 1998. p. 733-40.
24. Liu H, Boore DM, Joyner WB, Oppenheimer DH, Warrick RE, Zhang W, Hamilton JC, Brown LT. Comparison of phase velocities from array measurements of Rayleigh waves associated with microtremor and results calculated from borehole shear-wave velocity profiles. Bull Seism Soc Am. 2000; 90:666-78.
25. Satoh T, Kawase H, Iwata T, Higashi S, Sato T, Irikura K, Huang H. S-wave velocity structure of the Taichung basin, Taiwan, estimated from array and single-station records of microtremors. Bull Seism Soc Am. 2001; 91:1267-82.
26. Kudo K, Kanno T, Okada H, Ozel O, Erdik M, Sasatani T, Higashi S, Takahashi M, Yoshida K. Site-specific issues on strong ground motions during the Kocaeli, Turkey, earthquake of 17 August 1999. Bull Seism Soc Am. 2002; 92:448-65.
27. Ohori M, Nobata A, Wakamatsu K. A comparison of ESAC and FK methods of estimating phase velocity using arbitrarily shaped microtremor arrays. Bull Seism Soc Am. 2002; 92:2323-32.
28. Wathelet M. Array recordings of ambient vibrations: Surface-wave inversion [PhD thesis]. Belgium: University of Lige; 2005.
29. Davoodi M, Haghshenas E. Evaluating the Reliability of f-k and SPAC methods. Beijing, China: The 14th World Conference on Earthquake Engineering; 2008 Oct 12-17.
30. Zor E, Ozalaybey S, Karaaslan A, Cengiz T, Ozalaybey C, Tarancioglu A, Erkan B. Shear wave velocity structure of the İzmit Bay area (Turkey) estimated from active-passive array surface wave and single-station microtremor methods. Geophysical Journal International. 2010; 182(3):1603-18.
31. Esfahanizadeh M, Davoodi M, Haghshenas E, Jafari MK. Capability of F-K and SPAC methods in determining shear wave velocity of subsurface soil. Journal of Geotechnical Geology. 2014; 9(4):305-13.
32. Wathelet M, Jongmans D, Ohrnberger M. Surface wave inversion using a direct search algorithm and its application to ambient vibration measurements. Near Surf Geophys. 2004; 2:211-21.
33. Fah D, Kind F, Giardini D. A theoretical investigation of average H/V ratios. Geophys J Int. 2001; 145:535-49.
34. Wathelet M, Ohrnberger M, Cornou C. Sesarray package contents; 2005. Available from: <http://www.geophsy.org>